

USING WAVELET ENTROPY TO DISTINGUISH BETWEEN HUMANS AND DOGS DETECTED BY UWB RADAR

Yan Wang, Xiao Yu, Yang Zhang, Hao Lv, Teng Jiao,
Guo Hua Lu, Wen Zhe Li, Zhao Li, Xi Jing Jing,
and Jian Qi Wang*[†]

College of Biomedical Engineering, The Fourth Military Medical University, Xi'an 710032, China

Abstract—When using ultra-wide band (UWB) radar to detect targets in various conditions, identifying whether the target buried under building debris or in bad visibility conditions is a human or an animal is crucial. This paper presents the application of the wavelet entropy (WE) method to distinguish between humans and animal targets through brick wall and in free space at a certain distance. In the study, WE, WE change, and WE of the related range points were estimated for the echo signals from five humans and five dogs. Our findings indicate that the entropy or degree of disorder in the energy distribution of the human target was much lower than that of the dog, and the waveform of the human's entropy was smoother than that of the dog. In addition, the body micro motions of humans are much more ordered than those of dogs. WE can be employed as a quantitative measure for recognizing invisible targets and may be a useful tool in the UWB radar's practical applications.

1. INTRODUCTION

Ultra-wide band (UWB) is an attractive technology in different applications such as military industry, rescue missions, clinical medicine, etc. With its wide bandwidth and high spatial resolution, UWB radar can penetrate non-metallic objects, such as bricks, wood, dry walls, concrete and reinforced concrete. This allows for the

Received 25 March 2013, Accepted 25 April 2013, Scheduled 30 April 2013

* Corresponding author: Jian Qi Wang (wangjq@fmmu.edu.cn).

[†] The first two authors Yan Wang and Xiao Yu contributed equally to this work and should be regarded as co-first authors.

detection and localization of survivors buried under building debris after an earthquake, landslide, or fire [1–13].

The UWB radar can detect vital targets based on their periodic or non-periodic body movements or respiration, which means that both human and animal targets can be detected. Pets such as dogs living together with humans would probably be buried under rubbles after an earthquake. In this incident, as the trapped target's body movements are generally restricted, detection can be performed based mainly on the target's respiratory movements. The main methods to insure the presence or absence of vital targets are based on the periodic property of respiration or the certain frequency range of respiration [8, 13]. However, the respiratory rate of some animals such as dogs is similar to that of humans, which means only the detecting methods mainly used are useless in distinguishing between stationary humans and stationary animals. For the UWB radar system, identification and classification of vital signs are critically important in disaster rescue missions or surveillance. Searching for and rescuing more people in a timely manner is the key to a successful rescue after an earthquake. In an anti-terrorism mission, any anti-terrorism actions may be influenced if an animal's presence is not recognized properly. Therefore, unambiguous identification and classification of life targets are crucial for developing a UWB radar system for use in practical applications.

Current research primarily focuses on the use of UWB radar for vital signs detection, to detect and identify people buried underground, track moving human targets, or detect multi-stationary human targets [14–18]. The characteristics of animals detected by radar have also been studied [19, 20]. For example, [19] investigates different states of laboratory rats' movement activities. These studies aim to estimate laboratory animals' movement activities through a non-contact monitoring system, but not in detection applications.

Despite extensive research on propagation characteristics in humans and animals, few studies focus on the differences between the characteristics of radar echoes of humans and animals. In [21], the spectrograms of human targets were found to be different from that of other detected slow-moving targets, such as dogs. The difference in the modulation pattern due to the leg motion between the two was obvious. However, the difference in the spectrograms between the human and the dog based mainly on their different walking speed, which means the spectrogram method is not applicable in recognizing motionless targets in disaster search and rescue operations.

In [22], the UWB radar successfully detected a stationary person who held breathing detecting by his micro motions, which means the detector can detect a person based on his involuntary micro motions

that caused by physiological factors even if the person do not breath and not move. Therefore, the micro motions of targets can be the part and parcel to distinguish humans and animals. Considering a large part of the psychological effects and emotional and mental control, as well as additional undefined external influences, the reactions of humans and animals have their own characteristics, which means that body micro motions caused by the reactions of humans and animals also have their own characteristics, especially in incidents such as an earthquake disaster. With emotional and mental control, the reactions of humans are more rational than that of animals. Consequently, the micro motions of humans are more ordered compared with that of animals. According to the information theory, entropy is a relevant measure of order and disorder in a dynamic system, and can evaluate a complex signal quantitatively [23]. As non-stationary signals, the echoes caused by body motions are complex and vary in relation to time, amplitude, and frequency. Instantaneous changes of the echo signals caused by the body motions of humans and animals may also have their own rhythms. As a common tool used to analyze localized variations of non-stationary signals, wavelet analysis can provide an accurate temporal localization for the signal [24]. Therefore, entropy based on wavelet transform called wavelet entropy (WE) can quantify precisely time dynamics of order/disorder states of the echo signals [25]. The aim of this paper is to find the differences in WE between humans and dogs detected by the UWB radar.

The paper is organized as follows. Section 2 briefly describes the UWB system, which is implemented with low center frequency radar to ensure good penetration ability. Section 3 presents the pre-processing method and analyzes the obtained data. Section 4 describes the wavelet entropy processing method. Results from different experiments are shown in Section 5. Conclusions are drawn in Section 6.

2. UWB RADAR SYSTEM

The UWB radar setup is illustrated in Figure 1. The pulse generator produces trigger pulses with a pulse repetition frequency of 256 kHz. The pulses are sent to the transmitter and shaped into bipolar pulses to excite the transmitting antenna. The vertically polarized pulses are transmitted by the bow-tie dipole antenna with an average transmit power of about 5 mW. The reflected pulses are received by the receiving antenna which is identical to the transmitting antenna. In addition, the received pulses are sampled, integrated, and amplified, then stored as waveforms through the digital signal processor. The waveforms are sampled into 4096 points, and the recorded duration

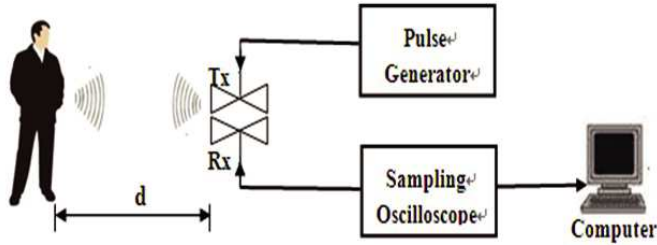


Figure 1. UWB radar setup.

is 40 ns. As to the electromagnetic theory, higher frequencies have higher spatial resolution; however, the system has weaker penetrating properties [13]. Considering practical applications such as earthquake rescue, the penetration ability must be taken into account. Therefore, the UWB system in this study was implemented with radar of low center frequency of 400 MHz, and the bandwidth of the received pulse is about 600 MHz.

3. SIGNAL PROCESSING AND ANALYSES

A stationary human and a stationary dog target, both located 3 m away from the antennas, were detected. According to [9], unwanted objects and noise produce a considerable amount of clutter in the acquired data. To obtain the targets' signals and accurately locate the targets, the measured data were pre-processed, and the power spectra were calculated, as shown in Figure 2. The magnitude of the power spectrum represents the power of signals in different ranges. A larger and more ordered signal indicates that the magnitude of the power spectrum is larger [10]. As shown in Figure 2, the respiration signal of the target is larger and more regular compared with random signals. Therefore, the maximum peak of the power spectrum corresponded to the location of the target. Figure 2(a) shows the power spectrum of the human target and indicates that the target's position was located accurately. The dog target's position can also be located accurately according to Figure 2(b). Although the magnitude of the human target's power spectrum was somewhat larger than that of the dog target, the magnitude of the power spectrum varied with the detecting environments. No other obvious difference was found between the power spectra of the human target and the dog target. Therefore, the power spectrum method is not a credible way to distinguish between humans and dog targets.

Figure 3 shows the spectra of the received signals. Figure 3(a) shows that the band spectrum of the human’s signal is narrow with a principal frequency of 0.23 Hz, whereas Figure 3(b) shows that the band spectrum of the dog’s signal is wider and has many high frequency components. The principal frequency of the band spectrum of the dog target’s signal is 0.24 Hz, which is almost the same as that of the human target. However, the components of the dog target’s signal were more complex. Despite some differences between the spectra of the signals of the human target and the dog target, the echo signals’ spectra depended on the detecting conditions and cannot be distinguished quantitatively.

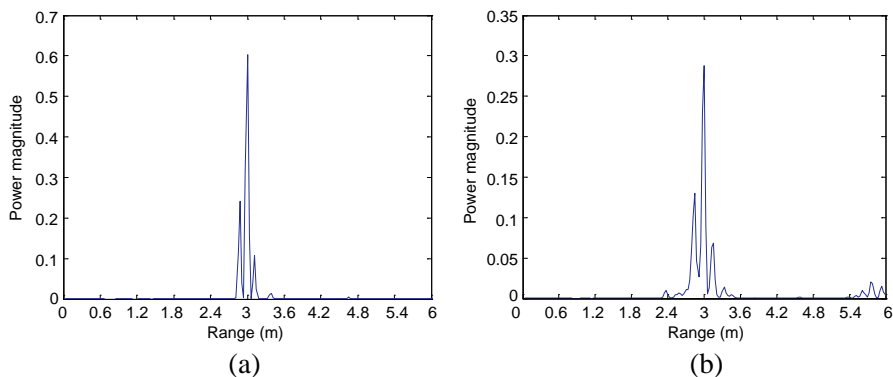


Figure 2. Power spectra of targets located 3m away from the antennas. (a) Power spectrum of the human target. (b) Power spectrum of the dog target.

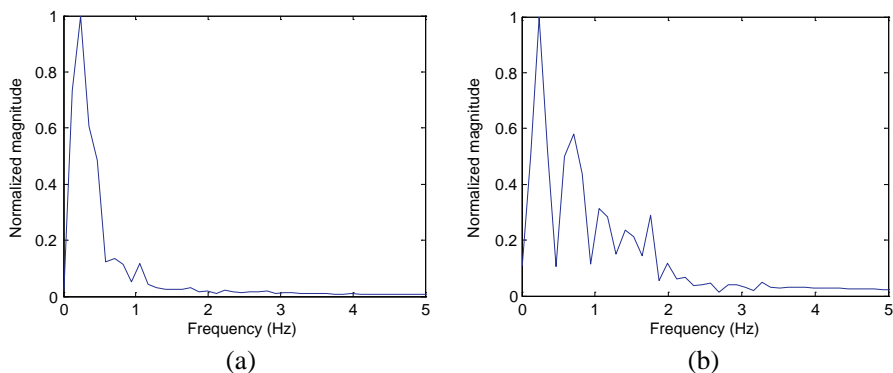


Figure 3. Spectra of the echo signals. (a) Spectrum of the human’s signal. (b) Spectrum of the dog’s signal.

4. WAVELET ANALYSIS

The above analysis indicates that the frequency components of the human and the dog targets differ to a certain extent. The dog target's signal had more complex components compared with that of the human target. Wavelet analysis can provide a time-frequency representation of the signal with optimal time-frequency resolution, and as a relevant measure of order or disorder in a dynamic system, entropy can quantify the signal's frequency components [23]. To better understand the time evolution of frequency patterns and quantify the degree of order of the echo signal, the entropy based on wavelet transform was used.

4.1. Wavelet Transform

Wavelet transform is a useful computational tool for a variety of signal applications. It was first introduced in 1984 by Grossmann and Morlet, and is an extension of the Fourier and Gabor transforms. Similar to Gabor transform, wavelet transform can decompose a signal in both time and frequency using a time window of varying widths; the wide windows correspond to low frequencies and the narrow windows to high frequencies. Consequently, the time-frequency resolution is high and accurate for all frequencies and can reveal the time evolution of frequencies in the analyzed signal.

The wavelet is a smooth and quickly vanishing oscillating function with good localization in both frequency and time. Morlet first considered wavelets as a family of functions generated by translations and dilations of a unique function called the "mother wavelet" $\psi(t)$. The family wavelet are defined as

$$\psi_{a,b}(t) = |a|^{-1/2} \psi\left(\frac{t-b}{a}\right) \quad a, b \in R, \quad a \neq 0 \quad (1)$$

where a is the scaling parameter or scale which measures the degree of compression, b the translation parameter which determines the time location of the wavelet, and t stands for time. If $|a| < 1$, then the wavelet in (1) is the compressed version of the mother wavelet and corresponds to higher frequencies. On the other hand, when $|a| > 1$, then $\psi_{a,b}(t)$ has a larger time-width than $\psi(t)$ and corresponds to lower frequencies. As a result, wavelets have time-widths and can adapt to their frequencies.

The continuous wavelet transform (CWT) of a signal $S(t) \in L^2(\mathfrak{R})$ is defined as the correlation between the series $S(t)$ with the family

wavelet $\psi_{a,b}$ for each a and b

$$\begin{aligned}
 W_s(a, b) &= \int_{-\infty}^{+\infty} S(t)\psi_{a,b}^*(t) dt = \langle S, \psi_{a,b} \rangle \text{ with } \psi_{a,b}(t) \\
 &= |a|^{-1/2}\psi\left(\frac{t-b}{a}\right)
 \end{aligned}
 \tag{2}$$

By selecting a special mother wavelet function $\psi(t)$ and the discrete set of parameters, $a_j = 2^{-j}$ and $b_{j,k} = 2^{-j}k$, with $j, k \in Z$, the wavelet family could be presented as

$$\psi_{j,k}(t) = 2^{j/2}\psi(2^j t - k) \quad j, k \in Z \tag{3}$$

The correlated discrete wavelet transform (DWT) of signal $S(t)$ can be obtained by

$$DWT_s(j, k) = \int_{-\infty}^{+\infty} S(t)\psi_{j,k}(t)dt = 2^{-j/2} \int_{-\infty}^{+\infty} S(t)\psi(2^{-j}t - k)dt \tag{4}$$

The DWT can provide a non-redundant representation of the signal, and the values constitute the coefficients in a wavelet series. These wavelet coefficients not only provide relevant information in a simple way but also provide a direct estimation of local energies at different scales. Furthermore, the information can be organized in a hierarchical scheme of nested subspaces which is called multiresolution analysis in $L^2(\mathfrak{R})$.

For practical signal processing, the signal is assumed to be given by the sampled values $S = \{s_0(n), n = 1, \dots, M\}$. According to the wavelet theories, the signal can be expressed as

$$S(t) = \sum_{j=-N}^{-1} \sum_k C_j(k) \psi_{j,k}(t) \tag{5}$$

where $j = -1, -2, \dots, -N$ is the number of resolution levels, and its maximum value is $N = \log_2(M)$ if the decomposition is carried out over all resolutions levels. $C_1(k), C_2(k), \dots, C_N(k)$ are the wavelet coefficients.

4.2. Relative Wavelet Energy

Orthogonal wavelet bases were used to decompose the signal. Therefore, the decomposed signals could be regarded as a direct estimation of local energies at different scales, and the wavelet coefficients can be given by $C_j(k) = \langle S, \psi_{j,k} \rangle$. Thus, the wavelet energy at resolution j can be defined as

$$E_j = \sum_k |C_j(k)|^2 \tag{6}$$

To study the temporal evolution of the above-defined quantifiers, the radar signal is divided among nonoverlapping temporal windows of length L . For each interval i ($i = 1, \dots, N_T$, with $N_T = M/L$), appropriate signal values are assigned to the central point of the time window. In case of diadic wavelet decomposition, the number of wavelet coefficients from all resolution levels is two times smaller than in the previous level. Here, the minimum length of the temporal window includes at least one coefficient at each level. By considering the mean wavelet energy instead of the total wavelet energy, the mean energy at each resolution level $j = -1, -2, \dots, -N$ for the time window i using the wavelet coefficients is

$$E_j^{(i)} = \frac{1}{N_j} \sum_{k=(i-1)L+1}^{iL} |C_j(k)|^2 \quad (7)$$

where N_j is the number of wavelet coefficients at resolution j included in the time window i .

As a result, the total energy of the wavelet coefficients at time window i can be obtained by

$$E_{total}^{(i)} = \sum_{j<0} E_j^{(i)} \quad (8)$$

Then, the relative wavelet energy, which represents the energy's probability distribution in scales, will be given by

$$p_j^{(i)} = E_j^{(i)} / E_{total}^{(i)} \quad (9)$$

Clearly, $\sum_j p_j^{(i)} = 1$ and the distribution $\{p_j^{(i)}\}$ is considered a time-scale density.

4.3. Wavelet Entropy

According to the Shannon entropy [23], which provides a measure of the information of any distribution for analyzing and comparing probability distribution, we define the temporal behavior of WE as [26]

$$H_{WT}^{(i)}(p) = - \sum_{j<0} p_j^{(i)} \cdot \ln [p_j^{(i)}] \quad (10)$$

To obtain a quantifier for the whole time period, the radar signal's mean WE can be defined as

$$H_{WT} = \frac{1}{N_T} \sum_{i=1}^{N_T} H_{WT}^{(i)} \quad (11)$$

Entropy is defined as a measure of uncertainty of the quantitative information in a system. The entropy value of a signal reflects the degree of complexity that the signal possesses. A more disordered signal indicates higher entropy [27]. Associating with the WT, which can be defined from a time-frequency representation of the signal, the entropy based on the WT, called WE, can provide additional information about the underlying dynamical process of the signal [28]. A periodic mono-frequency signal with a narrow band spectrum can be considered an ordered process, and its wavelet energy will be in one unique wavelet resolution. Consequently, its WE will be near zero or of a very low value. A totally random signal can represent a very disordered behavior and will have a wavelet representation with significant contributions from all frequency bands. Moreover, the wavelet energies will be almost equal for all resolution levels, thereby producing WE with maximal values.

4.4. Standard Deviation of Wavelet Entropy

In this study, the WE of the reflected signals based on the UWB radar was evaluated to reflect the body motion's rhythm associated with either body displacements or breathing. The non-stationary signal's frequency structure and the degree of order varied over time. Therefore, the WE of the signal fluctuated with time. To evaluate the entropy changes in relation to the mean entropy of the signal, the standard deviation of the WE was used as a measurable parameter, which can be defined as

$$S_{WT} = \left\{ \frac{1}{N_T} \sum_{i=1}^{N_T} \left(H_{WT}^{(i)} - H_{WT} \right)^2 \right\}^{\frac{1}{2}} \quad (12)$$

5. EXPERIMENTS AND RESULTS

The study involved 5 healthy humans aged between 22 and 25 years and 5 healthy dogs aged about 1 year who weighed between 20 kg and 25 kg. All dogs were provided by the Fourth Military Medical University.

Two experimental conditions were considered. In the first case, no obstacle was present between the targets and the antennas. In the second case, a 28 cm-thick brick wall was present between the targets and the antennas.

In the first case, each human target stood stationary with normal respiration 3 m away from the antennas. Each dog lay prone quietly on the experimental bench 3 m away from the antennas. In the second case, the states of the targets were the same as in the first case.

The targets were also located 3 m away from the antennas. A 28 cm-thick brick wall stood between the targets and the antennas. The experimental scenarios are shown in Figure 4.

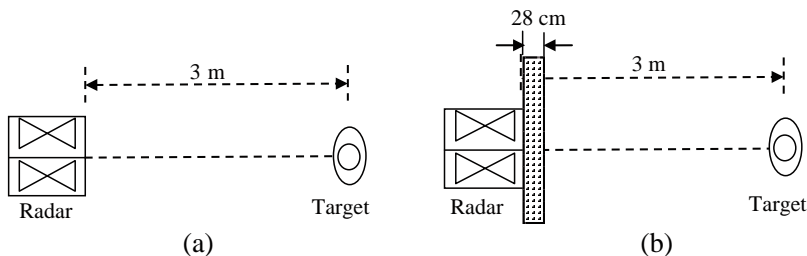


Figure 4. Scenarios for measuring targets using UWB radar. (a) Scenario for unobstructed case. (b) Scenario for obstructed case.

To quantitatively distinguish between humans and dog targets, the wavelet entropy was used on the radar signals to evaluate differences in complexity between humans and dogs. In the study, to contain at least one spectral coefficient from each frequency band, we used a time window length of 128 samples. As mentioned, in the UWB system, the received pulses were sampled into 4096 points. The maximum point of the power spectrum was regarded as the position of the target. A typical behavior of wavelet entropy over time is shown in Figure 5.

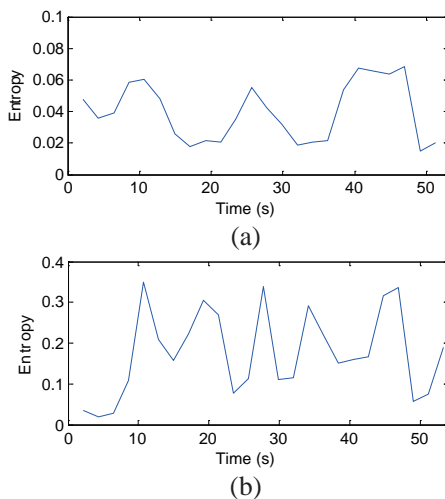


Figure 5. Time evolution of wavelet entropy corresponding to the signals of targets located 3 m away from the antennas. (a) Entropy of the human target. (b) Entropy of the dog target.

Figure 5 shows that the entropy value of both the human and the dog fluctuated as time progressed. Compared with the dog's entropy, the value of the human's entropy was much lower, and the amplitude was between 0.015 and 0.068, with a mean value of 0.04. The value of the dog's entropy fluctuated between 0.02 and 0.35, with a mean value of 0.18, which indicates that the entropy of the dog changed more significantly compared with that of the human. We used the mean WE value as the target's entropy. Figure 6 shows the mean WE values of the five humans and five dogs in the two experimental scenarios. The values of the dog targets' mean WE were higher than that of the human targets in the two scenarios. In both the obstructed and the unobstructed cases, the values of the five human targets' mean WE were between 0.02 and 0.08 and those of the five dog targets' mean WE were between 0.18 and 0.26. The WE values in the second case were higher in both human and dog targets. As Figure 7 shows, the signal in the obstructed case had more frequency components than that in the unobstructed case. This condition can be attributed to the clutter caused by the wall, which made the signals more complex.

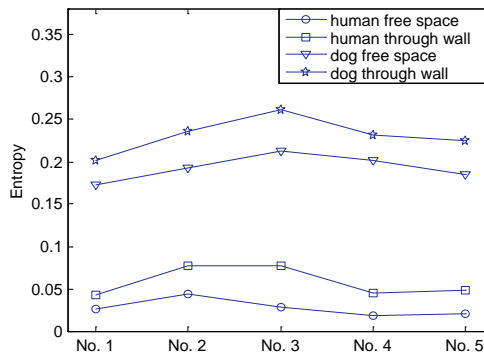


Figure 6. Mean wavelet entropy of five human targets in the unobstructed case (human free space), the obstructed case (human through wall), and five dog targets in the unobstructed case (dog free space) and the obstructed case (dog through wall).

To quantify the entropy changes, the standard deviations of the WE of the five humans and the five dogs are shown in Figure 8.

As Figure 8 illustrates, the standard deviation of the human's WE was smaller than that of the dog in the obstructed and unobstructed cases. The changes of WE of the human and the dog differed significantly in the two experimental cases, which suggests that the WE of the human displayed almost constant values unlike that of the dog. No obvious difference between the standard deviations of WE

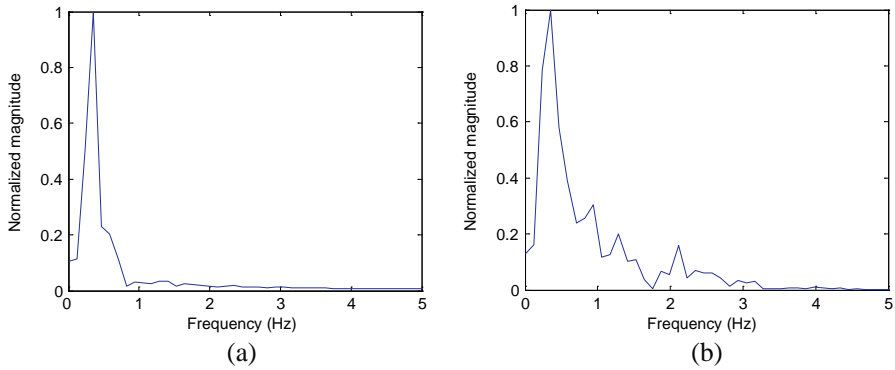


Figure 7. Spectra of a human target in both unobstructed and obstructed cases. (a) Spectrum in the unobstructed case. (b) Spectrum in the obstructed case.

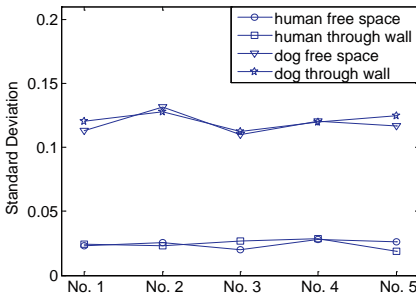


Figure 8. Standard deviations of the WE of the five human targets in the unobstructed case (human free space) and the obstructed case (human through wall), and of five dog targets in the unobstructed case (dog free space) and the obstructed case (dog through wall).

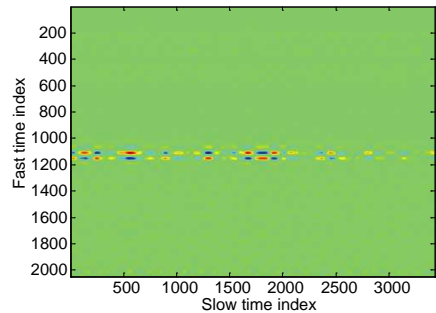


Figure 9. Data matrix received from the target located 3 m away from the antennas.

was observed in the two experimental cases. Combined with Figures 5 and 8, the changes in the time evolution of WE in the human’s signal were smaller than those in the dog’s signal. Therefore, the human’s and the dog’s signals differed significantly.

According to the observation and the analysis of the data, the echo signals of targets fluctuated not just in one point, but over a certain range, as shown in Figure 9.

We compressed the 4096 points along the fast time index which associated to range into 2048 points [18]. As Figure 9 shows, the target located in the 1100 point. The target signal and its adjacent signals had high correlation coefficients [13]. The obtained reflected signal was caused by the target’s skin and internal organ movements or the movements of other parts of the body, which is why the scope of the target’s movements was not just fixed in one point. Figure 10 illustrates the entropies of the echo signals’ 201 points before and after the targets’ position for 100 points. Entropies of both the human and the dog target were periodic functions, and the cycle was approximately 40. Figure 11 illustrates a cycle of the entropies of the echo signals’ 41 points before and after the targets’ position for 20 points. As Figure 11(a) shows, the value of the human target’s entropy in the first case was quite low, with a value below 0.05. The entropies of the points before and after the target’s point for 15 points were at the same level with the target’s points. The human target’s entropy had a regular and smooth shape. Figure 11(b) shows the dog target’s entropy in the first case. The value of the dog’s entropy was above 0.15, and some points’ mean WE had the same value as the target’s point. However, the scope was much smaller than that of the human. The shape of the dog target’s entropy was not as smooth as that of the human. The entropies of the targets in the second scenario are shown in Figures 11(c) and 11(d). The figures show that the entropies in the obstructed case were a little higher than in the unobstructed case in both the human and the dog targets, with a value above 0.05 in the human and a value above 0.2 in the dog target. The entropy of the human target was also much lower

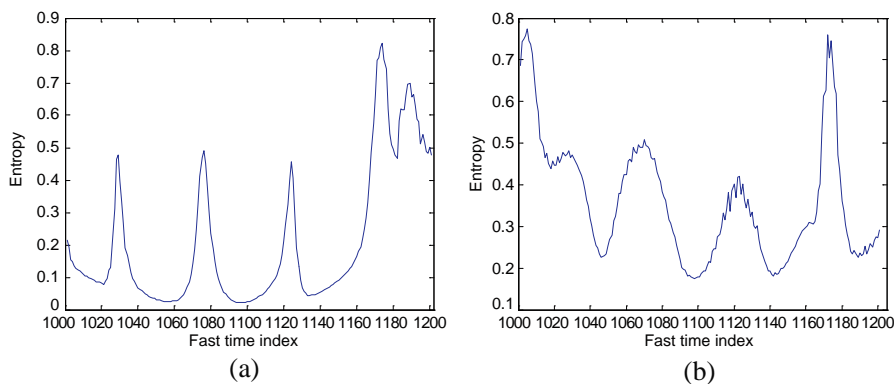


Figure 10. Entropy of the echo signals’ 201 points before and after the targets’ position for 100 points. (a) Entropy of the human target. (b) Entropy of the dog target.

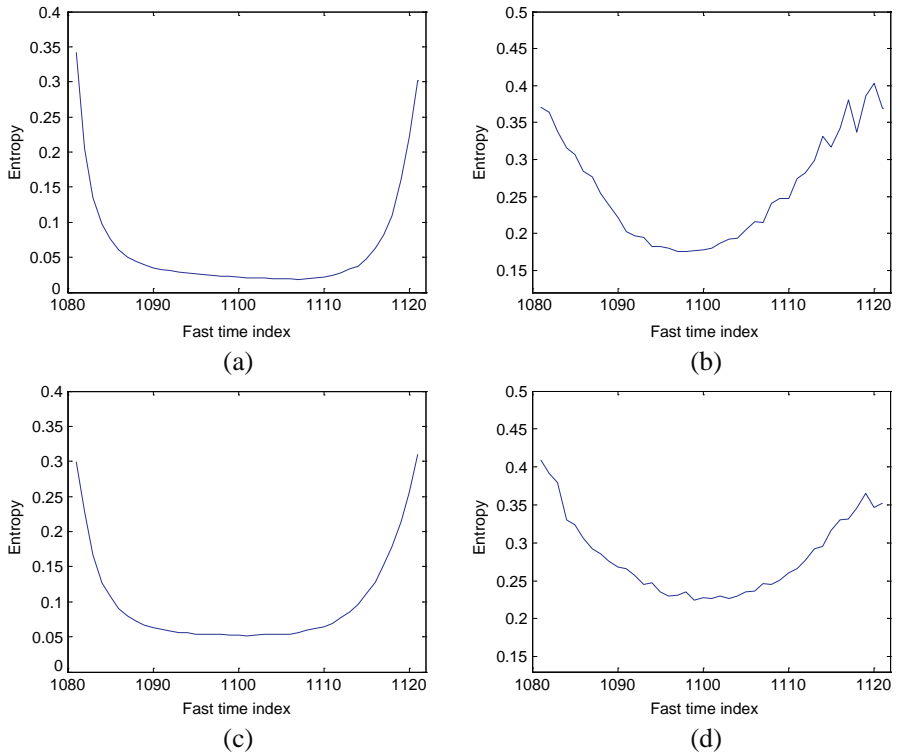


Figure 11. Entropy of the echo signals' 41 points before and after the targets' position for 20 points. (a) Entropy of the human target in the first case. (b) Entropy of the dog target in the first case. (c) Entropy of the human target in the second case. (d) Entropy of the dog target in the second case.

than that of the dog target, which indicates that the echo signals of the human targets were more ordered than those of the dog targets. The components of the dogs' echoes were more complex and diverse than those of the humans.

6. CONCLUSION

This study described the use of quantitative parameters derived from wavelet transform in the analysis of the returned signals obtained by an UWB radar to investigate the difference between human targets and dog targets. The wavelet entropy can detect changes in a non-stationary signal due to the localization characteristics of the wavelet

transform and provided information about the degree of order or disorder associated with the reflected signal. The standard deviation of the WE evaluated the degree of WE changes. In addition, the time evolution of these quantifiers provided information about the dynamics associated with the targets echo signals.

In the study, the entropies of the targets in different scenarios were analyzed. The human's signal exhibited a more rhythmic and ordered behavior which is compatible with the dynamical process of the dog's signal in both obstructed and unobstructed scenarios. The wavelet entropies' characteristics of humans' signals did not appear to change significantly, according to the standard deviation of the WE. The differences in entropies between humans and dogs may be due to the structures of the different bodies. Based on the property of electromagnetic waves, the electromagnetic wave pulses emitted by radar are scattered from a boundary of two media with different parameters [29]. For a target that has a complex shape, the echo UWB radar signal consists of multipath components as the incident UWB pulse scatters independently from different body parts at different times with different amplitudes. This behavior is dependent on the distance to the body part and the size, shape, and composition of the scattering part [30]. In addition, the movement of an animal during wakefulness increases the power of the signal at low frequencies and produces irregular waveforms, even in a resting state and during rapid eye movement sleep [31]. This movement may cause the complexity of the animal's signal, whereas the human's movement is more ordered due to the control of emotion and mentality. The wavelet entropy in the obstructed case was higher compared with that in the unobstructed case, which is related to the presence of wall clutter which increased the signal's complexity. As the scope of the target's motion was not just limited to one point, a particular range has the same WE level as the target's point. In addition, our findings indicate that the body motion amplitude of the animal was smaller than that of the human. The findings of this study facilitate the differentiation of human targets and animal targets through the use of the UWB radar. The improved performance of the UWB radar system allows the UWB radar to meet the requirements of real-world applications.

ACKNOWLEDGMENT

This work was supported by the National Science and Technology Support Program of China (Grant No. 2012BAI20B02), and the Natural Science Foundation of Shaanxi Province (Grant No. 2012JM4047). The authors express their gratitude to M. Liu,

Q. An and Y. Tian for their valuable assistance on data acquisition and manuscript preparation, and Y. F. Li for his excellent software development support.

REFERENCES

1. Zhu, F., S. C. S. Gao, A. T. S. Ho, T. W. C. Brown, J. Li, and J. D. Xu, "Low-profile directional ultra-wideband antenna for see-through-wall imaging applications," *Progress In Electromagnetics Research*, Vol. 121, 121–139, 2011.
2. Sun J. and M. Li, "Life detection and location methods using UWB impulse radar in a coal mine," *Mining Science and Technology (China)*, Vol. 21, 687–691, 2011.
3. Shaban, H. A., M. Abou El-Nasr, and R. M. Buehrer, "Reference range correlation (RRcR) ranging and performance bounds for on-body UWB-based body sensor networks," *Progress In Electromagnetics Research B*, Vol. 35, 69–85, 2011.
4. Conceicao, R. C., M. O'Halloran, M. Glavin, and E. Jones, "Numerical modelling for ultra wideband radar breast cancer detection and classification," *Progress In Electromagnetics Research B*, Vol. 34, 145–171, 2011.
5. Lazaro, A., D. Girbau, and R. Villarino, "Wavelet-based breast tumor localization technique using a UWB radar," *Progress In Electromagnetics Research*, Vol. 98, 75–95, 2009.
6. Zheng, W., Z. Zhao, and Z. Nie, "Application of TRM in the UWB through wall radar," *Progress In Electromagnetics Research*, Vol. 87, 279–296, 2008.
7. Desrumaux, L., M. Lalande, J. Andrieu, V. Bertrand, and B. Jecko, "An innovative radar imaging system based on the capability of an UWB array to steer successively in different directions," *Progress In Electromagnetics Research B*, Vol. 32, 91–106, 2011.
8. Liu, Z., L. Liu, and B. Barrowes, "The application of the Hilbert-Huang transform in through-wall life detection with UWB impulse radar," *PIERS Online*, Vol. 6, No. 7, 695–699, 2010.
9. Lv, H., G. H. Lu, X. J. Jing, and J. Q. Wang, "A new ultra-wideband radar for detecting survivors buried under earthquake rubbles," *Microwave and Optical Technology Letters*, Vol. 52, No. 11, 2621–2624, 2010.
10. McGinley, B., M. O'Halloran, R. C. Conceicao, G. Higgins, E. Jones, and M. Glavin, "The effects of compression on ultra

- wideband radar signals,” *Progress In Electromagnetics Research*, Vol. 117, 51–65, 2011.
11. Sharafi, A. and A. Ahmadian, “Respiration-rate estimation of a moving target using impulse-based ultra wideband radars,” *Australas Phys. Eng. Sci. Med.*, Vol. 35, 31–39, 2012.
 12. Crowgey, B. R., E. J. Rothwell, L. C. Kempel, and E. L. Mokole, “Comparison of UWB short-pulse and stepped-frequency radar systems for imaging through barriers,” *Progress In Electromagnetics Research*, Vol. 110, 403–419, 2010.
 13. Li, Y. F., X. J. Jing, H. Lv, and J. Q. Wang, “Analysis of characteristics of two close stationary human targets detected by impulse radio UWB radar,” *Progress In Electromagnetics Research*, Vol. 126, 429–447, 2012.
 14. Jia. Y., L. Kong, and X. Yang, “A novel approach to target localization through unknown walls for through-the-wall radar imaging,” *Progress In Electromagnetics Research*, Vol. 119, 107–132, 2011.
 15. Lazaro, A., D. Girbau, and R. Villarino, “Analysis of vital signs monitoring using an IR-UWB radar,” *Progress In Electromagnetics Research*, Vol. 100, 265–284, 2010.
 16. Zhang, W., A. Hoorfar, and L. Li, “Through-the-wall target localization with time reversal music method,” *Progress In Electromagnetics Research*, Vol. 106, 75–89, 2010.
 17. Tian, B., D. Y. Zhu, and Z. D. Zhu, “A novel moving target detection approach for dual-channel SAR system,” *Progress In Electromagnetics Research*, Vol. 115, 191–206, 2011.
 18. Li, W. Z., Z. Li, H. Lv, G. H. Lu, Y. Zhang, X. J. Jing, S. Li, and J. Q. Wang, “A new method for non-line-of-sight vital sign monitoring based on developed adaptive line enhancer using low centre frequency UWB radar,” *Progress In Electromagnetics Research*, Vol. 133, 535–554, 2013.
 19. Anishchenko, L. N., A. S. Bugaev, S. I. Ivashov, and I. A. Vasiliev, “Application of bioradiolocation for estimation of the laboratory animals’ movement activity,” *PIERS Online*, Vol. 5, No. 6, 551–554, 2009.
 20. Donohue, K. D., D. C. Medonza, E. R. Crane, and B. F. O’Hara, “Assessment of a non-invasive high-throughput classifier for behaviours associated with sleep and wake in mice,” *BioMedical Engineering Online*, Vol. 7, No. 1, 1–14, 2008.
 21. Otero, M., “Application of a continuous wave radar for human gait recognition,” *Proceedings of SPIE, Signal Processing, Sensor*

- Fusion and Target Recognition*, Vol. 5809, 538–548, 2005.
22. Yarovoy, A. G., L. P. Ligthart, J. Matrzas, and B. Levitas, “UWB radar for human being detection,” *IEEE Aerospace and Electronic Systems Magazine*, Vol. 23, No. 5, 36–40, May 2008.
 23. Shannon C. E., “A mathematical theory of communication,” *Bell System Technical Journal*, Vol. 27, 379–423, Jul. 1948; 623–656, Oct. 1948.
 24. Blanco S., A. Figliola, R. Quian Quiroga, O. A. Rosso, and E. Serrano, “Time-frequency analysis of electroencephalogram series (III): Wavelet packets and information cost function,” *Physical Review E*, Vol. 57, 932–940, 1998.
 25. Rosso, O. A., S. Blanco, J. Yordanova, V. Kolev, A. Figliola, M. Schürmann, and E. Basar, “Wavelet entropy: A new tool for analysis of short time brain electrical signals,” *Journal of Neuroscience Methods*, Vol. 105, 65–75, 2001.
 26. Yordanova, J., V. Kolev, O. A. Rosso, M. Schurmann, O. W. Sakowitz, M. Ozgoren, and E. Basar, “Wavelet entropy analysis of event-related potentials indicates modality-independent theta dominance,” *Journal of Neuroscience Methods*, Vol. 117, 99–109, 2002.
 27. Al Nashash, H. A., “Wavelet entropy for subband segmentation of EEG during injury and recovery,” *Annals of Biomedical Engineering*, Vol. 31, 653–658, 2003.
 28. Quiroga, R. Q., O. A. Rosso, and E. Basar, “Wavelet entropy: A measure of order in evoked potentials,” *Electr. Clin. Neurophysiol.*, Vol. 49, 298–302, 1998.
 29. Immoreev, I. and S. Ivashov, “Remote monitoring of human cardio-respiratory system parameters by radar and its applications,” *Ultrawideband and Ultrashort Impulse Signals*, 34–38, Sevastopol, Ukraine, Sep. 15–19, 2008.
 30. Singh, S., Q. Liang, D. Chen, and S. Li, “Sense through wall human detection using UWB radar,” *EURASI Journal on Wireless Communications and Networking*, Vol. 2011, No. 20, 1–11, 2011.
 31. Zeng, T., C. Mott, D. Mollicone, and L. D. Sanford, “Automated determination of wakefulness and sleep in rats based on non-invasively acquired measures of movement and respiratory activity,” *Journal of Neuroscience Methods*, Vol. 204, 276–287, 2012.